Energy-Harvesting Microsensors: Low-Energy Task Schedule & Fast Drought-Recovery Design

Andrés A. Blanco, *Graduate Student Member, IEEE,* and Gabriel A. Rincón-Mora, *Fellow, IEEE*
Georgia Institute of Technology, Atlanta, Georgia, 30332-0250 U.S.A
E-mail: ablanco@gatech.edu and Rincon-Mora@gatech.edu

***Abstract*—The main challenge with microsensors is limited space, because tiny batteries store little energy. Harvesting energy helps, but only when ambient energy is available. And even then, power is low because miniaturized transducers harness little power. This is why managing how and when to schedule functional tasks is so important. This paper proposes a schedule that requires the battery to hold only the energy necessary to sustain single events and allows the battery to drain across harvesting droughts. When input power returns, an inefficient starter charges a temporary supply that bootstraps the system quickly into an efficient state. This way, when harvested input, idle, and peak load power are 10, 0.5, and 1000 µW, a 0.7% efficient starter and an 87% efficient charger can recharge a 1.8-µF battery to 1 V in 220 ms with a 71-pF temporary supply and in 13 s without the temporary supply. The system therefore wakes 59× faster than without a temporary supply and 1880× faster and with 1800× less capacitance than when forcing the battery to survive a 2-hour power outage.**

Keywords*—*Energy-drought recovery, energy harvesting, low-energy task schedule, microsensor, microsystem, startup, wake.

I. Energy-Harvesting and Drought-Recovering Wireless Microsystems

Wireless microsensors can add life-, cost-, and energy-saving intelligence to, among others, homes, hospitals, biological systems, vehicles, factories, and farms [1]–[5]. Key to their ubiquity is miniaturization because space in modern and emerging applications is increasingly scarce. Tiny onboard batteries, however, store little energy, and in the case of super capacitors, also leak considerable power [6]. So harnessing ambient energy is often a requirement for these microsystems.

Still, ambient energy E_A is not always available [7]–[8]. And when available, miniaturized transducers might only avail 1 of the 1000 $\mu W/mm^2$ that the highest power-producing devices can [3], [5]. So with E_A, the harvesting source v_H in Fig. 1 feeds a maximum power-point (MPP) charger that replenishes a battery C_B with enough energy to supply the system. The power supply [9]–[10] then draws and conditions power to satisfy the sensor, digital-signal processor (DSP), power amplifier (PA), and other system components. The central processor (CP) assesses the state of the system to determine which blocks to activate and which to disable.

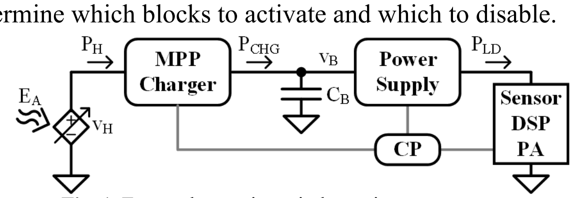

Fig. 1. Energy-harvesting wireless microsensor system.

Since v_H does not always output power P_H, C_B must be large enough to store the energy that the system requires across harvesting droughts. Or if allowed to drain, which is more practical because drought periods can be long and super capacitors leak, the system should recover fast enough when E_A returns to leverage what P_H avails before E_A again fades.

Critical design considerations here are size and wake time. But for a small C_B, load power should be low. This is why Section II proposes a low-energy "just-enough" task schedule. A small C_B, however, drains across harvesting droughts. So Sections III and IV propose, analyze, and assess how the system should enter and recover from power outages.

II. Low-Energy "Just-Enough" Task Schedule

To minimize how much energy the battery C_B supplies, the system should schedule no more than one task at a time. And a task should only occur when C_B has enough energy to sustain it. In a microsensor, sensing and processing what is being sensed constitute one such task and transmitting processed data another. Of these, transmissions usually require more energy with E_T than sensing events do with E_S. So depending on the application, a system can sense and process more data by sensing N times before every transmission.

For this, the system can monitor C_B's voltage v_B as a way of determining when C_B stores enough energy to sustain a task. And as soon as C_B collects sufficient energy, the system executes a task. So when the harvester charges C_B to sensing threshold $V_{S(TH)}$, like Fig. 2 indicates and Fig. 3 shows at 180 ms, the system senses, processes, and stores data. The sensor and microelectronics involved in this process discharge C_B below $V_{S(TH)}$. And when v_B again reaches $V_{S(TH)}$ at 200 ms, the system senses again and the sequence repeats (and loops in Fig. 2) the N times that the application requires.

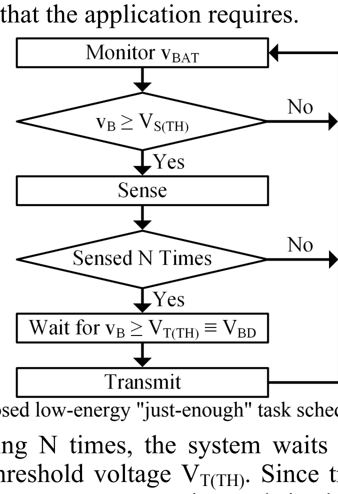

Fig. 2. Proposed low-energy "just-enough" task schedule flow chart.

After sensing N times, the system waits until v_B reaches transmission threshold voltage $V_{T(TH)}$. Since transmissions are usually the most power-consuming task in the system, $V_{T(TH)}$ corresponds to the highest energy level that C_B should hold. The smallest C_B that will hold this energy will do so at the highest voltage possible, which corresponds to the breakdown voltage V_{BD} of the circuit. So when v_B reaches V_{BD}, which happens at 350 ms in Fig. 3, the PA transmits the information collected across N sensing events.

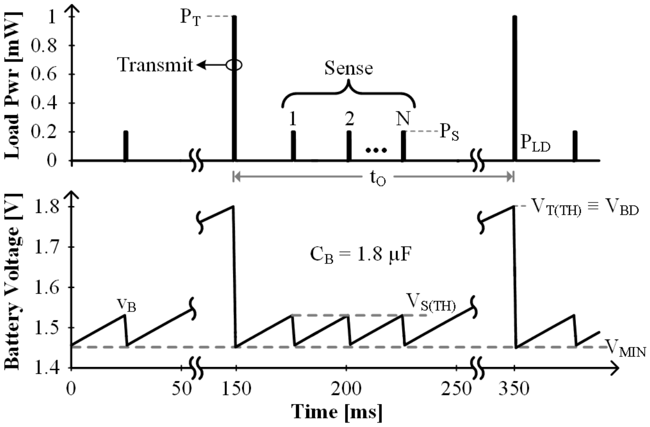

Fig. 3. Power train and corresponding battery-voltage simulation.

Each event should discharge C_B to no less than the energy and corresponding voltage required V_{MIN} to sustain offline tasks. This is why v_B drops to V_{MIN} after every transmission and sensing event in Fig. 3. By waiting for v_B to reach sensing and transmission thresholds $V_{S(TH)}$ and $V_{T(TH)}$, the system automatically adjusts the time t_O between transmissions to keep average load power $P_{LD(AVG)}$ and power losses P_{LOSS} at the level the harvesting source v_H supplies with P_H:

$$P_H = P_{LD(AVG)} + P_{LOSS} . \quad (1)$$

The application and the state of the art of supporting technologies dictate the thresholds and values required to operate the system. CMOS circuits, for example, can sustain up to 1.8–4.5 V and consume 11 nW when idling, 2–50 μJ when sensing, and 38 nJ–58 μJ when transmitting [1]–[2], [4]–[5], as Table I shows. Chargers can deliver 0.15%–0.7% of the power drawn from a 40–500 mV source during startup and 87% from higher voltages in steady state [11]–[13]. Although startup does not affect the time C_B requires to charge when enough ambient energy is present (in Fig. 3), low startup efficiency extends the time needed to recover from harvesting droughts.

TABLE I. POWER LEVELS IN THE STATE OF THE ART

Parameter		Range	Reference
Harvesting Source	v_H	40–500 mW	[12]
Harvesting Source Power	P_H	1–1000 μW/mm^2	[3] and [5]
Idle Power	P_{IDLE}	11 nW	[2]
Sense Energy	E_S	2–50 μJ	[1] and [4]
Transmission Energy	E_T	38 nJ–58 μJ	[4]–[5]
Breakdown Voltage	V_{BD}	1.8–4.5 V	[11]
Startup Efficiency	η_{ST}	0.15%–0.7%	[12]
Steady-State Efficiency	η_{SS}	87%	[13]

III. DOWNTIME OPERATION, ANALYSIS, AND DESIGN

The charger in Fig. 1, like most harvesting chargers [13], monitors the power it delivers with P_{CHG} to adjust and ensure it operates at its maximum power point (MPP). When this P_{CHG} falls below the minimum operating threshold P_{TH} in Fig. 4, the PA transmits a system-offline report. The central processor (CP) then disables the power supply that feeds the sensor, DSP, PA, and other blocks until P_{CHG} climbs back to P_{TH}. But if P_{CHG} falls further to zero, v_H's harvesting power P_H is no longer able to sustain charger losses. So CP shuts the charger to enter standby or sleep mode until v_H recovers to the minimum level $V_{H(MIN)}$ from which the charger can draw and output power.

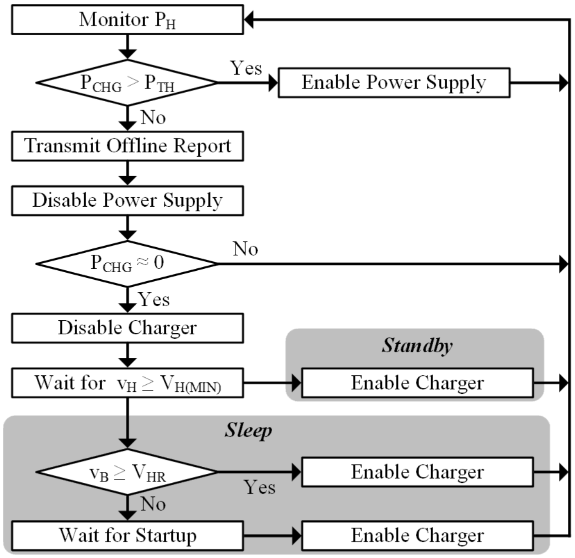

Fig. 4. Proposed downtime flow chart.

A. Standby

When designed for standby, the battery C_B is large enough to keep v_B from ever falling below the headroom level V_{HR} that the charger requires to operate. This way, the charger can recover efficiently from a harvesting drought. Although almost nothing is on during the outage, low-power survival blocks in CP still operate, so C_B nevertheless discharges, albeit slowly. Self-discharge in C_B accelerates this process. So when the PA sends an offline transmission at 0.25 s in Fig. 5, the PA discharges C_B quickly and survival blocks continue to discharge C_B after that until the drought ends at 7200 s.

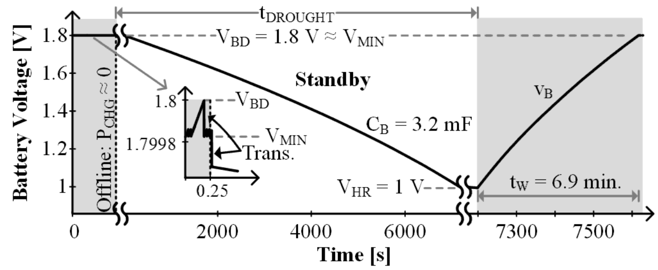

Fig. 5. Standby simulation.

Just before sending an offline report at 0.25 s, C_B should store enough $0.5C_Bv_B^2$ energy above V_{HR} to sustain the transmission E_T and supply survival blocks E_Q and C_B's self-leakage E_{LK} across the longest possible drought, which can be hours or longer [7]. But since the drought can begin just after a transmission starts, C_B should hold another E_T. So to minimize the space C_B occupies, v_B at this point can be near the breakdown voltage V_{BD} of the circuit. This way, C_B can be 3.2 mF when E_T is 1 μJ, E_Q's P_Q is 0.5 μW and E_{LK}'s P_{LK} is negligibly lower, T_{ON} is 2 hours, V_{BD} is 1.8 V, and V_{HR} is 1 V:

$$C_B \equiv \frac{2E_T + E_Q + E_{LK}}{0.5\left(V_{T(TH)}{}^2 - V_{HR}{}^2\right)} = \frac{2E_T + P_QT_{ON} + P_{LK}T_{ON}}{0.5\left(V_{BD}{}^2 - V_{HR}{}^2\right)} . \quad (2)$$

Wake: After the drought, when v_H is back at or above $V_{H(MIN)}$, CP enables the charger whose output raises v_B above V_{HR}. The system then waits across wake time t_W until C_B has enough $0.5C_B(V_{MIN}^2 - V_{HR}^2)$ energy above V_{HR} at V_{MIN} to send an offline transmission and supply survival blocks P_Q and C_B's self-leakage P_{LK} across another drought, which can be near 1.8 V when C_B is 3.2 mF, E_T is 1 µJ, P_Q is 0.5 µW and P_{LK} is negligibly lower, T_{ON} is 2 hours, and V_{HR} is 1 V:

$$V_{MIN} = \sqrt{\frac{E_T + P_Q T_{ON} + P_{LK} T_{ON}}{0.5C_B} + V_{HR}^2}. \quad (3)$$

CP also waits for P_{CHG} to reach P_{TH} to enable the power supply, and in so doing, bring the system back online. Since the charger delivers a $P_H\eta_{SS}$ portion of P_H, where η_{SS} is steady-state efficiency, v_B can reach V_{MIN} in 6.9 minutes when C_B is 3.2 mF, V_{MIN} is 1.8 V, V_{HR} is 1 V, P_H is 10 µW, and η_{SS} is 87%:

$$t_W = \frac{0.5C_B\left(V_{MIN}^2 - V_{HR}^2\right)}{P_{CHG}} = \frac{0.5C_B\left(V_{MIN}^2 - V_{HR}^2\right)}{P_H\eta_{SS}}. \quad (4)$$

B. Sleep

When designed for sleep, C_B can drain completely. C_B should therefore hold the energy needed to sustain an offline transmission E_T and supply survival blocks P_Q and C_B's self-leakage P_{LK} across a transmission period T_T. But since the drought can begin just after a transmission starts, C_B should hold another E_T. This time, however, T_T is so short that E_Q and E_{LK} are negligible. So to minimize the space C_B occupies, v_B can be at V_{BD}. C_B can therefore be 1.8 µF when E_T is 1 µJ, T_{ON}'s T_T is 1 ms, P_Q is 0.5 µW, V_{BD} is 1.8 V, and V_{HR} is 1 V.

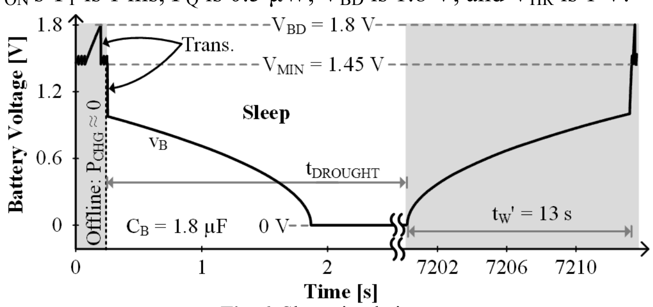

Fig. 6. Sleep simulation.

<u>Wake</u>: Like in standby, CP enables the charger after the drought. When C_B collects the energy for an offline transmission and P_{CHG} reaches P_{TH}, CP enables the power supply and the system. The difference here is, C_B charges from 0 V, not from V_{HR}. This means, the charger must, initially, derive power from v_H, which can be so low at 40–500 mV that startup efficiency η_{ST} is often less than 0.7% [12], [14]–[15].

In other words, the charger first delivers a $P_H\eta_{ST}$ fraction of P_H to raise v_B to V_{HR} and then a $P_H\eta_{SS}$ portion to raise v_B to V_{MIN} [14]. So with 1.8 µF, for example, V_{MIN} is 1.45 V when E_T is 1 µJ and V_{HR} is 1 V, where T_{ON} is zero. t_W' can therefore be 13 s when P_H is 10 µW, η_{ST} is 0.7%, and η_{SS} is 87%:

$$t_W' = \frac{0.5C_B V_{HR}^2}{P_H\eta_{ST}} + \frac{0.5C_B\left(V_{MIN}^2 - V_{HR}^2\right)}{P_H\eta_{SS}}. \quad (5)$$

<u>Temporary Supply</u>: One way to accelerate the wakeup process is to keep the charger above its minimum headroom level V_{HR} with a smaller temporary battery C_T.[12], [15] This way, C_T charges quickly above V_{HR}, and with more than V_{HR} feeding the charger, the charger is more efficient and therefore faster. C_T, however, should only feed the charger until v_B reaches V_{HR} because, at and above V_{HR}, C_B can do the rest.

To be more specific, C_T supplies gate-drive and quiescent power P_C lost in the controller, which is a P_Hk_C portion of the P_H drawn. Across one switching cycle T_{SW}, C_T should therefore store above V_{HR} this controller energy E_C or P_CT_{SW}:

$$C_T \equiv \frac{E_C}{0.5\left(V_{BD}^2 - V_{HR}^2\right)} = \frac{P_H k_C T_{SW}}{0.5\left(V_{BD}^2 - V_{HR}^2\right)}. \quad (6)$$

Resistances, however, consume another P_Hk_R fraction. So of the $P_H - P_Hk_R$ delivered, C_T receives P_Hk_C and C_B charges with $P_H - P_Hk_R - P_Hk_C$ or P_{CB}. C_B in Fig. 7 therefore charges with P_{CB} to V_{HR} in $t_{B(HR)}$, across which time C_T recharges N times:

$$N = \frac{t_{B(HR)}}{T_{SW}} = \frac{0.5C_B V_{HR}^2}{T_{SW}P_{CB}} = \frac{0.5C_B V_{HR}^2}{T_{SW}\left(P_H - P_Hk_R - P_Hk_C\right)}. \quad (7)$$

Unfortunately, Ohmic losses are higher when using C_T because the charger passes more power at P_H than without C_T at $P_H - P_Hk_C$, so η_{SS} with C_T is $(P_Hk_C)k_R/P_H$ or k_Ck_R lower: $\eta_{SS} - k_Ck_R$.

When first waking with startup efficiency η_{ST}, however, C_T should charge just high enough above V_{HR} to supply E_C:

$$V_{T1} = \sqrt{\frac{E_C}{0.5C_T} + V_{HR}^2} = \sqrt{\frac{P_H k_C T_{SW}}{0.5C_T} + V_{HR}^2}. \quad (8)$$

So when waking, C_T charges to V_{T1} with $P_H\eta_{ST}$ and C_B first charges to V_{HR} with P_{CB} or $P_H(\eta_{SS} - k_Ck_R)$ and then to V_{MIN} with P_{CHG} or $P_H\eta_{SS}$:

$$t_W'' = \frac{0.5C_T V_{T1}^2}{P_H\eta_{ST}} + \frac{0.5C_B V_{HR}^2}{P_H\left(\eta_{SS} - k_Ck_R\right)} + \frac{0.5C_B\left(V_{MIN}^2 - V_{HR}^2\right)}{P_H\eta_{SS}}. \quad (9)$$

Following the same example, C_T, N, V_{T1}, and wake time t_W" can be 71 pF, 1040, 1.8 V, and 220 ms when T_{SW} is 100 µs and k_C and k_R in η_{SS} are 8% and 5%.

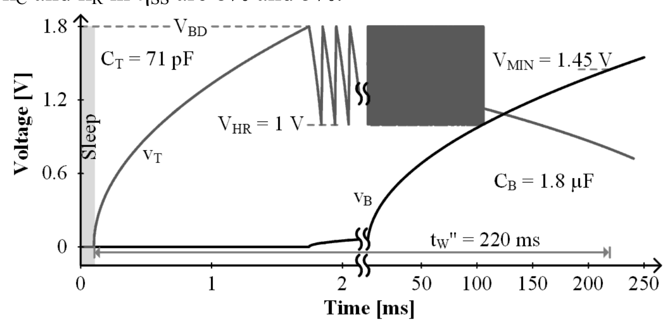

Fig. 7. Wake simulation with and without temporary supply C_T.

IV. Design Tradeoffs

Although modern survival circuits consume very little power, they still discharge the battery C_B across long harvesting droughts [16]. Super capacitors suffer more because they also leak [6]. Unfortunately, keeping C_B charged above the minimum headroom level V_{HR} that circuits need to operate across these outages requires substantial capacitance, and as a result, volume and wake time, as Fig. 8 states. This is why sleep mode saves space, because while asleep, C_B can drain. This way, C_B and wake time can be 1800× and 1880× lower after a 2-hour drought when allowed to sleep than when kept in standby.

The challenge with sleeping is waking with a drained C_B and a millivolt source. This is because chargers output less than 0.7% of the power drawn when supplied from 40–500-mV [12]. The problem with this is a long wake period. A smaller temporary battery C_T can help because C_T charges quicker, and with C_T's v_T above V_{HR}, the charger is more efficient (at 87% [13]) and therefore faster. This way, C_T delivers the energy lost in the controller. In the example cited, wake time is 59× times shorter with only 0.004% more capacitance for C_T.

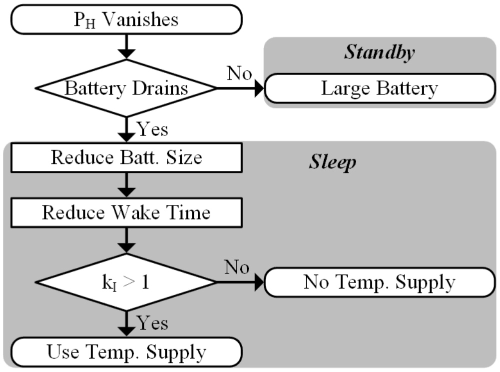

Fig. 8. Wake design flow chart.

In practice, startup efficiency η_{ST} determines wake time t_W' without C_T, steady-state efficiency η_{SS} sets the counterpart t_W" with C_T, and k_Ck_R's reduction in t_W" is normally insignificant. Wake improvement factor k_I with C_T therefore reduces to

$$k_I \equiv \frac{t_W'}{t_W''} \approx \left(\frac{\eta_{SS}}{\eta_{ST}}\right)\left(\frac{V_{HR}}{V_{MIN}}\right)^2. \tag{10}$$

In other words, improvement k_I hinges on how much η_{SS} overwhelms η_{ST} and how little V_{MIN} surpasses V_{HR}. Because with lower η_{SS}, the losses that C_T supplies climb, so C_B receives less power. And with a higher V_{MIN}, C_B requires more time to charge. This is why C_T reduces wake time (i.e., k_I exceeds 1) in Fig. 9 when η_{SS}/η_{ST} outweighs $(V_{MIN}/V_{HR})^2$ and k_I is 59× in the example cited, which represents a typical case.

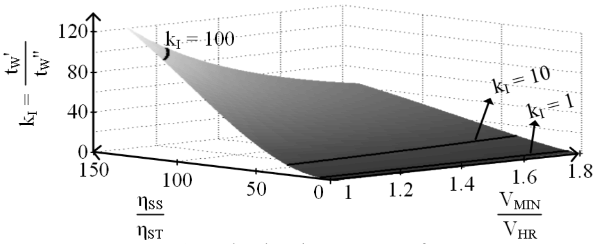

Fig. 9. Wake-time improvement factor.

V. CONCLUSIONS

To keep onboard batteries small, microsystems should perform only one task at a time, and do so as soon as stored energy is sufficient to sustain a task. And when ambient energy vanishes, the system should stand by or sleep. This paper proposes an algorithm and a design that allow microsystems to sleep and reduce battery size by 1800× and wake time by 1880×. With only 0.004% additional capacitance for a temporary battery, the system wakes 59× faster from a no-charge condition. This way, with the low-energy "just-enough" schedule, analytical methods, and design process proposed here, smaller energy-harvesting sensor systems can sustain more events more frequently and recover from harvesting droughts more quickly.

ACKNOWLEDGEMENT

The authors thank Texas Instruments for sponsoring this research and Paul Emerson and Dr. Orlando Lazaro for their mentorship and support.

REFERENCES

[1] D. F. Lemmerhirt and K. D. Wise, "Chip-Scale Integrations of Data-Gathering Microsystems", *Proceedings of IEEE*, vol. 94, pp. 1138-1159, June 2006.

[2] Y. Lee, S. Bang, I. Lee, Y. Kim, M. H. Ghaed, P. Pannuto, P. Dutta, D. Sylvester, and D. Blaauw, "A Modular 1 mm^3 Die-Stacked Sensing Platform with Low Power I^{2}C Inter-Die Communication and Mutli-Modal Energy Harvesting", *IEEE Journal of Solid-State Circuits*, vol. 48, pp. 229-243, January 2013.

[3] B. A. Warneke, M. D. Scott, B. S. Leibowitz, L. Zhou, C. L. Bellew, J. A. Chediak, J. M. Kahn, B. E. Boser, and K. S. J. Pister, "An Autonomous 16 mm^3 Solar-Powered Node for Distributed Wireless Sensor Networks", *Proceedings of IEEE Sensors*, vol. 2, pp. 1510-1515, June 2002.

[4] M. Flatscher, M. Dielacher, T. Herndl, T. Lentsch, R. Matischek, J. Prainsack, W. Pribyl, H. Theuss, and W. Weber, "A Bulk Acoustic Wave (BAW) Based Transceiver for and In-Tire-Pressure Monitoring Sensor Node", *IEEE Journal of Solid-State Circuits*, vol. 45, pp. 167-177, January 2010.

[5] G. Chen, H. Ghaed, R. u. Haque, M. Wieckowski, Y. Kim, G. Kim, D. Fick, D. Kim, M. Seok, K. Wise, D. Blaauw, and D. Sylvester, "A Cubic-Millimeter Energy-Autonomous Wireless Intraocular Pressure Monitor," *IEEE Int. Solid-State-Circuits Conf. Digest of Technical Papers (ISSCC)*, pp 310-312, February 2011.

[6] H. Yang and Y. Zhang, "Analysis of Supercapacitor Energy Loss for Power Management in Environmentally Powered Wireless Sensor Nodes", *IEEE Trans. on Power Electronics*, vol. 28, pp. 5391-5403, November 2013.

[7] M. L. Ku, Y. Chen, and K. J. R. Liu, "Data-Driven Stochastic Models and Policies for Energy Harvesting Sensor Communications", *IEEE* J. on Selected Areas in Communications, vol. 33, pp. 1505-1520, August 2015.

[8] P. Lee, Z. A. Eu, M. Han, and H. P. Tan, "Empirical modeling of a solar-powered energy harvesting wireless sensor node for time-slotted operation," *IEEE Wireless Communications and Networking Conference*, pp 179-184, March 2011.

[9] S. Bader and B. Oelmann, "Short-term Energy Storage for Wireless Sensor Networks Using Solar Energy Harvesting," *IEEE Conf. on Sensing and Control*, pp 71-76, April 2013.

[10] M. Seok, S. Hanson, M. Wieckowski, G. K. Chen, Y. S. Lin, D. Blaauw, and D. Sylvester, "Circuit Design Advances to Enable Ubiquitous Sensing Environments," *IEEE Int. Symp. on Circuits and Systems*, pp 285-288, May 2010.

[11] S. Kim and G. A. Rincón-Mora, "Efficiency of Switched-indcutor DC-DC Converter ICs across Process Technologies," *IEEE Int. Symp. on Circuits and Systems*, pp 460-463, May 2012.

[12] A. A. Blanco and G. A. Rincón-Mora, "A 44-93 µs 250-400-mv 0.18-µm CMOS Starter for DC-Sourced Switched-Inductor Energy Harvesters", *IEEE Trans. on Circuits and Systems II*, vol. 61, pp. 1002-1006, December 2014.

[13] Y. Qiu, C. Van Liempd, B. O. het Veld, P. G. Blanken and C. Van Hoof, "5µW-to-10mW input power range inductive boost converter for indoor photovoltaic energy harvesting with integrated maximum power point tracking algorithm," *IEEE Int. Solid-State-Circuits Conf. Digest of Technical Papers (ISSCC)*, pp 118-120, February 2011.

[14] P. Chen, *et al.*, "An 80 mV Startup Dual-Mode Boost Converter by Charge-Pumped Pulse Generator and Threshold Voltage Tuned Oscillator with Hot Carrier Injection," *IEEE J. of Solid-State Circuits*, vol. 47, pp. 2554–2562, Nov 2012.

[15] Y.K. Ramadass and A.P. Chandrakasan, "A Battery-Less Thermoelectric Energy Harvesting Interface Circuit with 35 mV Startup," *IEEE J. of Solid-State Circuits*, vol. 46, pp. 333–341, January 2011.

[16] Y. Lee, G. Chen, S. Hanson, D. Sylvester, and D. Blaauw, "Ultra-low Power circuit techniques for a new class of sub-mm^3 sensor nodes," *IEEE Custom Integrated Circuits Conf. (CICC)*, September 2010.